Schizophrenia Bulletin vol. 35 no. 1 pp. 32–46, 2009
doi:10.1093/schbul/sbn149
Advance Access publication on November 20, 2008

Brain-Performance Correlates of Working Memory Retrieval in Schizophrenia: A Cognitive Modeling Approach

Gregory G. Brown[2], Gregory McCarthy[3], Amanda Bischoff-Grethe[4], Burak Ozyurt[4], Doug Greve[5], Steven G. Potkin[6], Jessica A. Turner[6], Randy Notestine[4], Vince D. Calhoun[7], Judy M. Ford[8], Daniel Mathalon[8], Dara S. Manoach[5], Syam Gadde[9], Gary H. Glover[10], Cynthia G. Wible[11], Aysenil Belger[12], Randy L. Gollub[5], John Lauriello[13], Daniel O'Leary[14], and Kelvin O. Lim

[2]Department of Psychiatry, University of California San Diego; Psychology Service, VA San Diego Healthcare System; [3]Department of Psychiatry, Yale University; [4]Department of Psychiatry, University of California San Diego; [5]Department of Psychiatry, Massachusetts General Hospital; [6]Department of Psychiatry, University of California Irvine; [7]Electrical and Computer Engineering; The Mind Research Network, University of New Mexico, Albuquerque, NM 87131; [8]Department of Psychiatry, University of California San Francisco; [9]Department of Psychiatry, Duke University; [10]Radiological Sciences Laboratory, Stanford University; [11]Department of Psychiatry, Harward Medical School and Brockton VAMC; [12]Department of Psychiatry, University of North Carolina—Chapel Hill; [13]Department of Psychiatry, University of New Mexico; [14]Department of Psychiatry, University of Iowa; [15]Department of Psychiatry; Minneapolis VA Medical Center, University of Minnesota

Correlations of cognitive functioning with brain activation during a sternberg item recognition paradigm (SIRP) were investigated in patients with schizophrenia and in healthy controls studied at 8 sites. To measure memory scanning times, 4 response time models were fit to SIRP data. The best fitting model assumed exhaustive serial memory scanning followed by self-terminating memory search and involved one intercept parameter to represent SIRP processes not contributing directly to memory scanning. Patients displayed significantly longer response times with increasing memory load and differed on the memory scanning, memory search, and intercept parameters of the best fitting probability model. Groups differed in the correlation between the memory scanning parameter and linear brain response to increasing memory load within left inferior and left middle frontal gyrus, bilateral caudate, and right precuneus. The pattern of findings in these regions indicated that high scanning capacity was associated with high neural capacity among healthy subjects but that scanning speed was uncoupled from brain response to increasing memory load among schizophrenia patients. Group differences in correlation of the best fitting model's scanning parameter with a quadratic trend in brain response to increasing memory load suggested inefficient or disordered patterns of neural inhibition among individuals with schizophrenia, especially in the left perirhinal and entorhinal cortices. The results show at both cognitive and neural levels that disordered memory scanning contributes to deficient SIRP performance among schizophrenia patients.

Key words: schizophrenia/item recognition/functional magnetic resonance imaging/stochastic models

Introduction

Understanding the brain substrate of cognitive impairment is a fundamental project for neurobiological theories of schizophrenia. Investigators have advanced deficit models[1] or inefficiency models to explain dysfunctional brain-behavior organization among individuals with schizophrenia.[2] Deficit models assume that impaired cognitive functioning in schizophrenia is caused by the diminished neural activity of unresponsive neurons.[1] Inefficiency models assume that when mildly impaired to normal performance is observed among individuals with schizophrenia, performance will be associated with the increased neural activity of neurons with reduced computational power.[2] When used to interpret the results from functional brain imaging studies, the 2 models are not mutually exclusive in that some cognitive task conditions might elicit deficient functioning whereas others might elicit inefficient functioning.

To investigate the relationship between task performance and brain activity in schizophrenia, investigators have manipulated experimental variables related to cognitive function and/or have plotted the association of brain activity with performance.[2,3,20] When brain activity is plotted against performance, a simple deficit model predicts the same regression curve for individuals with schizophrenia as found among healthy individuals. The difference in the plots of patient and healthy comparison groups would appear as a greater concentration

[1]To whom correspondence should be addressed; tel: 858-246-06-7, fax: 858-552-7414, e-mail: gbrown@ucsd.edu.

of patients at the low performance/low activity end of the curve. A simple inefficiency model accounts for the brain-behavior functioning of individuals with schizophrenia by assuming a leftward shift of the accuracy/activity curve found among healthy individuals.[19,66] For schizophrenia patients and healthy individuals who respond at the same level of performance, a leftward shift in the patient group would predict increased amounts of brain activity among some individuals with schizophrenia. Simple models assume that the association of performance with brain activation has the same shape and direction among individuals with schizophrenia as observed among those without. It is theoretically important, therefore, that performance-activity plots obtained from some studies have revealed patterns of correlation that are qualitatively different among individuals with schizophrenia compared with healthy participants.[2,3] Neither the simple deficit model nor the simple inefficiency model predict these differential patterns of correlation.

Correlations between performance and brain activity have enriched the database that neurobiological theories of schizophrenia need to explain. Yet, interpretations of these correlations are limited by the complexity of the cognitive tasks used and by the complexity of the brain's response to cognitive challenges. Possibly, different cognitive components of complex tasks might be related to neural activity in different brain areas, whereas brain activity itself might change as task demands change over trials. A variety of specialized experimental designs, such as event-related or trial-based designs, exist to decompose the brain's response to changing task demands into separate epochs.[4,5] Multivariate techniques, such as independent components analysis, can also decompose the temporal signal from functional imaging studies into spatiotemporal components of brain response.[6,7] Yet, these specialized designs and multivariate techniques have their focus on decomposing the brain's response and have contributed less to the decomposition of cognitive function into theoretically meaningful components.

In this study, we used probability models to decompose global response times (RTs) into processing times related to component cognitive functions underlying working memory (WM) retrieval on an item recognition paradigm.[8,9] WM impairment appears to be a core neuropsychological deficit among individuals with schizophrenia.[10–12] Deficits in WM have been reported in medication-naive, first-episode schizophrenia patients and persist throughout the course of the disorder.[13] Compromised WM performance predicts poorer community outcome and impaired skill learning more successfully than do positive psychotic symptoms.[14,15] Impaired WM performance is also observed among individuals with a genetic risk of schizophrenia, suggesting that WM dysfunction contributes to an individual's vulnerability to the disorder, in addition to its contribution to a patient's disability.[16–18]

This study examined cognitive processes underlying memory load effects on a fixed-set variant of the Sternberg item recognition paradigm (SIRP). The task involved the presentation of a memory set that included 1, 3, or 5 digits followed by 14 probe digits. Participants responded manually to indicate whether or not a probe digit was included in the memory set just studied. Because it encompassed a large number of probe trials, the multiprobe, fixed-set design efficiently assessed the brain's response to memory probe events under different memory load conditions. We chose to study the SIRP because findings of abnormal brain response among individuals with schizophrenia have been replicated for SIRP tasks, increasing the likelihood of finding meaningful correlations between cognitive function and brain activity.[2,20] The task has also previously been used in behavioral studies to investigate short-term WM functioning among groups of patients with schizophrenia.[23–29]

An important challenge to correlating performance from this task with brain activity is that performance is determined by several cognitive processes related to stimulus encoding, memory access, decision making, and response selection and execution.[8,9] When memory load is manipulated, as in functional brain imaging studies of individuals with schizophrenia, the memory access stage of processing becomes the primary process of interest. For investigators interested in performance/brain activity correlations, it would be desirable to have a measure of memory access separate from measures of other cognitive functions involved in the task. There is a long history of modeling the RTs obtained from SIRP-type tasks, providing several well-validated probability models useful in decomposing global RTs into theoretically meaningful components processes.[8,9] One well-validated SIRP finding is that RTs are generally a linear function of the memory set size.[9] The linearity supports the strategy of assigning separate cognitive functions to the RT line's slope from the cognitive functions assigned to the line's intercept on the ordinate axis.[8,9] The slope component is often assumed to reflect a short-term WM scanning process with all processing unrelated to memory load affecting the intercept value.[8,9] When considering different memory scanning models, it is useful to plot RT by memory set size for positive trials—when the target probe is included in the memory set—separately from negative trials—when the target probe is not included in the memory set. One intuitive model for accessing memory set items assumes that the target probe is serially compared or scanned with each member of the memory set. Once a match occurs, the individual terminates the search.[8] This serial, self-terminating model has been well studied and, despite its intuitive appeal, does not often fit group data.[8] Typically, the self-terminating search model does not simultaneously fit the RT slopes of both negative and positive trials. Alternative models have questioned the self-terminating assumption leading to the exhaustive

serial search model that generally fits positive and negative slopes better. Other alternatives have questioned the serial assumption leading to parallel processing models that predict similar or different slope patterns from the predictions of the serial exhaustive model, depending on the architecture of the particular parallel model.[9]

Although the multiprobe, fixed-set design of our SIRP task increased its efficiency when detecting the brain's response to memory probes, the length of the probe period might have introduced episodic recognition processes into the set of mechanisms that determine performance. Models that combine memory scanning with episodic memory search have been studied in healthy individuals.[21] To increase the range of predictions that our models can make, we evaluated a hybrid memory scanning/search model, which assumes that a memory search occurs after memory scanning is complete. Presumably, memory search is a strategy individuals use to recheck the validity of the decision based on memory scanning. Rechecking has been advanced in lexical retrieval models to account for evidence of combined effects of automated and expectancy mechanisms on lexical decision times.[22] The lexical decision results show that even when tasks are performed at high accuracy under time pressure, subjects will use multiple sources of information to make decisions prior to responding.[22] We extend this principle of multifactorial decision making to our analysis of the SIRP by introducing the concept of rechecking into the hybrid model. Of particular interest for our study is that the hybrid model was the only model we considered that predicted convergent slopes between negative and positive RT curves (see below).

We studied 4 SIRP RT models to select the best fitting model to decompose RTs into component RTs. These processes would be reflected in model parameters that separate the overall RT into measures of memory scanning speed; encoding, response selection, and response execution speed; and, possibly, memory search speed. To test hypotheses about group differences in performance/brain activity correlations, we fit the best fitting model to each participant's RT data in order to obtain model parameter estimates on a case-by-case basis. Our aim was to estimate separate memory scanning and memory search speeds from the speeds of other cognitive processes involved in the SIRP. We then correlated the memory scanning and memory search parameters with measures of blood oxygen level–dependent (BOLD) response obtained during a functional magnetic resonance imaging (fMRI) scan while subjects performed the SIRP. Given the findings of abnormal brain activation to increasing memory load among individuals with schizophrenia in the prefrontal cortex (PFC),[19,20] we anticipated group differences in the correlation of the best fitting model's memory scanning parameter with BOLD response to increasing memory load in the PFC. This hypothesis assumes that the abnormal brain response observed at the group level will mediate some of the variation in level of impairment within the patient group and that this mediation is different from that observed among healthy participants. Because a previous event-related fMRI study has found that PFC activation was exclusively associated with the SIRP's probe period,[53] we focus our analysis on BOLD data obtained during the memory probe period.

Methods

Participants

One hundred and two outpatients with *Diagnostic and Statistical Manual of Mental Disorders, Fourth Edition* (*DSM-IV*),[30] diagnoses of schizophrenia or schizoaffective disorder and 103 healthy comparison subjects, matched groupwise on age and gender to the patients, were recruited at each of 8 sites throughout the United States. Recruitment targets aimed for equal numbers of patients and comparison subjects to be enrolled from each site. To be included in the study, individuals needed to be between the ages of 18 and 70 years, be fluent in English, and have normal hearing and natural or correctable eyesight sufficient to read the visual display in magnet rooms. Individuals were excluded from the study if they had a contraindication to MRI, a current major neurological or medical illness, previous head injury with loss of consciousness greater than 30 minutes, substance and/or alcohol dependence, an estimated IQ score less than 75 as measured by the North American Adult Reading Test (NAART),[31] or were being treated for migraines. Individuals with hypertension could be studied provided their blood pressure was controlled. Patients were excluded if they met criteria for *DSM-IV* diagnoses other than schizophrenia or schizoaffective disorder or had significant extrapyramidal symptoms or tardive dyskinesia as predetermined by movement scale results (see scales below). Schizophrenia patients were required to be clinically stable with no significant changes in their psychotropic medications in the previous two months. Comparison subjects were excluded if they had a current or past psychiatric disorder or if a first-degree family member had a diagnosis of a psychotic illness. All sites received local institutional review board approval for this study.

Clinical Assessment and Scales

Prior to the onset of the study, a study investigator experienced in the assessment of schizophrenia (J.L.) trained clinical raters on the administration of the clinical scales and the Structured Clinical interview for DSM-IV axis I disorders (SCID-1, patient with psychotic screen and non-patient editions).[32] All participants received the SCID, a demographics questionnaire, the Edinburgh Handedness Inventory,[33] Socioeconomic Status Questionnaire,[34] the NAART,[31] Simpson Angus Scale,[67] the Barnes Akathisia Scale,[68] and the Abnormal Involuntary

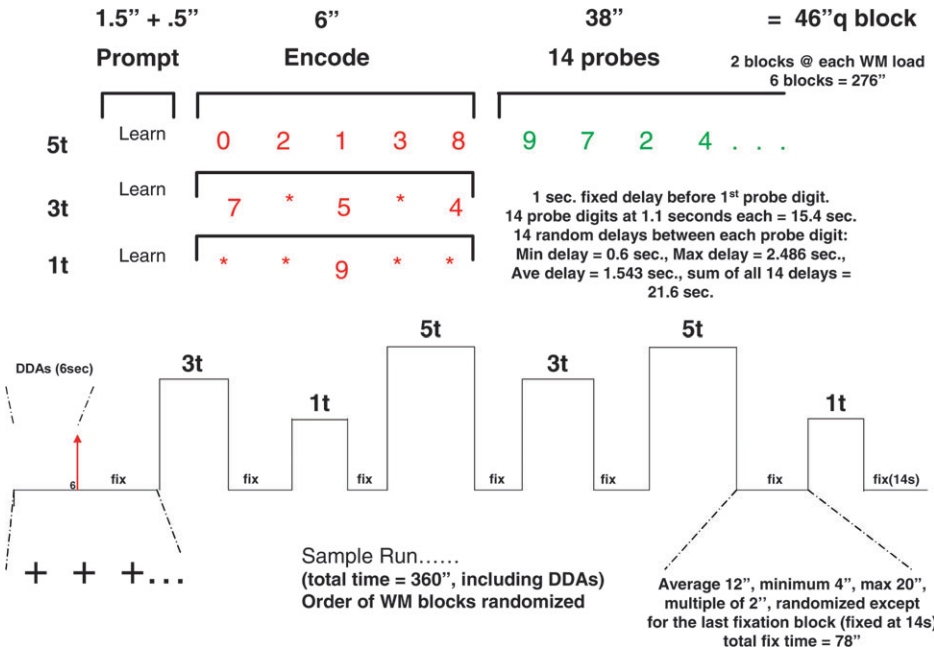

Fig. 1. Each Run of the Item Recognition Paradigm Included 6 Blocks. Each block was composed of a prompt; an encode period when a memory set composed of 1, 3, or 5 digits was presented; a probe period; and interleaved fixation periods. Blocks included only one memory set with each memory set size presented twice per run. The prompt was the word "Learn," which was presented for 1.5 seconds. Following 0.5 seconds of blank screen, the memory set was presented for 6.0 seconds. A blank screen lasting 1.0 second appeared between encode and probe period. Each of the 14 probes was presented for 1.1 seconds followed by a jittered blank screen interval lasting 1.543 seconds on the average. The minimum duration for the blank screen was 0.6 seconds, and the maximum was 2.486 seconds. Jittered intervals were selected so that the total probe interval always equaled 38 seconds. A flickering cross-hair appeared during a jittered fixation period, which lasted 12.0 seconds on the average and ranged from 4.0 seconds to 20 seconds.

Movement Scale.[35] In addition, all patients received symptom ratings on Scales for the Assessment of Positive Symptoms and Negative Symptoms (SANS).[36]

Sternberg Item Recognition Paradigm

This fixed-set, item recognition task was programmed in E-Prime version 1.1.4.1 (Psychology Software Tools, Pittsburgh, PA, Inc). Each 360-second SIRP run was composed of 6 blocks of memory items separated by fixation blocks (figure 1). During a run, 2 memory sets for each memory set size were presented twice. Stimuli were visually presented using the projection method standard at each site. Each memory block was composed of a prompt, an encode epoch, and a probe epoch. The 1.5-second prompt cued subjects to learn the subsequent memory set composed of 1, 3, or 5 digits presented during the encode period for 6 seconds. The 38-second probe period was composed of 7 positive trials where the probe digit was a member of the memory set just presented randomly intermixed with 7 negative trials. Responses were recorded on a SRBox response device.[65] Both accuracy and RTs were recorded. Three runs were acquired with the order of presentation of the memory set sizes varied across the runs. Participants responded to 42 positive and 42 negative probes over all trials associated with a particular memory set size. See the caption to figure 1 for more details about task timing including how probe target presentation was jittered. The task was pilot tested and refined in a group of individuals with schizophrenia in order to create a task that they could perform at high accuracy.

Image Acquisition

Images were acquired from 8 magnet sites (1.5T Picker, 1.5T, Siemens, for 3.0T Soemens, 3T General Electric, 4T General Electric) that performed the same protocol. After obtaining a sagittal localizer scan to confirm head placement, a T_2-weighted structural scan was obtained in the oblique axial, anterior commissure - posterior commissure (AC-PC) plane using a fast spin echo or turbo spin echo sequence (field of view [FOV] = 22 cm, 27 slices, 4 mm slice with 1 mm skip, repetition time/echo time (TR/TE) = 5000/68 ms, echo train length or turbo factor = 12 or 13, 256 × 192 matrix, total scan time = 1:30 min). Five Siemens sites collected field maps to create voxel-shift maps to correct for image distortions in areas of high magnetic inhomogeneity.[37] The field map protocol (from Massachusetts General Hospital) collected magnitude and phase contrast in separate scans at a bandwidth of +100 kHz or equivalent 64 × 64 matrix with scan plane = oblique axial, FOV = 22 cm, 27 slices, 4 mm slice thickness with 1 mm skip, TR = 500 or 1000 ms if a body coil was used, TE1 = minimum full, TE2 = TE1 + 4.84 milliseconds (1.5T), 2.46 milliseconds (3T), 1.75 milliseconds (4T), and flip angle = 55° (3T/4T) or 65° (1.5T).

Time series of T_2*-weighted images were obtained while participants performed 3 runs of the SIRP (pulse sequence = echoplanar image or spiral single-shot gradient echo protocol, scan plane = oblique axial AC-PC, FOV = 22 cm, 27 slices, 4 mm slice thickness with 1 mm skip, TR = 2000 ms, TE = 30 ± 2 ms (3T/4T), 40 ± 2 ms (1.5T), flip angle = 90°, 64 × 64 matrix). For each of the 3 runs, 3 dummy acquisitions were programmed into the sequence followed by 177 active frames.

Next, a high resolution, 3D T_1-weighted scan was obtained using an inversion-recovery prepared, fast spoiled gradient-recalled sequence at General Electric sites and a magnetization-prepared rapid acquisition gradient echo sequence at Siemens sites (scan plane = sagittal, FOV = 22 × 22 cm, 256 × 192 matrix, 160–170 slices, 1.2 mm slice thickness, TR/TE = 2300/2.99, flip angle = 9°, scan time = 7–9 min. The slice prescription at the Picker site was FOV = 24 cm, 256 × 256 matrix, 120 slices, 1.2 mm slice thickness, TR/TE = 1300/3.7, flip angle = 20°. Within each session, additional runs were performed to obtain functional brain data associated with an auditory oddball task, a sensorimotor task, and a breath hold task. These data will be presented elsewhere.

In order to share images across sites, locally stored images were registered with the Storage Resource Broker (SRB)[38] using upload scripts and procedures developed by the Function Biomedical Informatics Research Network (fBIRN). Upload scripts were developed not only to register locally stored images but also to create XCEDE XML files containing image characteristics and to convert images into the NIfTI-1 format.[39]

Image Analysis

Images were processed with a developmental version of the fBIRN Image Processing System (FIPS), an image analysis pipeline primarily using routines from the FMRIB Software Library (FSL).[40] In the version of FIPS used here, preprocessing steps were separated from the remainder of the FIPS pipeline, with XML and related files developed to track provenance information. The preprocessing scripts used FSL's MCFLIRT to motion correct the time series of each subject (aligning to the middle volume), PRELUDE and FUGUE to B_0 correct images at sites where field maps were collected, and "slicetimer" to correct images for slice-timing differences.[40] To equilibrate images for potential site differences in the BOLD signal due to spatial smoothness, we smoothed all 3D volumes to 8-mm full width at half maximum (FWHM).[41] The smooth-to script used FSL's "betfunc" program to skull-strip the fMRI dataset, then Freesurfer's "mri_fwhm" program[42] to iteratively determine the appropriate width for the smoothing kernel and FSL's "ip" program to spatially smooth the fMRI dataset to the prescribed smoothness.

Image Quality Assurance Screening. Because this federated imaging database was created while upload scripts, the fBIRN quality assurance tool, SRB directory structures, and the NIfTI format were still being developed and tested, some upload and file format errors occurred. These errors were identified by checking for incomplete datasets, examining the content of the XCEDE XML files that accompanied uploaded NIfTI images, by checking image header information and by visual inspection of the images. Typical errors involved missing files, incorrect slice number, slice order, timing, or orientation information. Once problems were identified, scripts were written to repair NIfTI and XCEDE XML files on a case-by-case basis, as required.

Mapping Functional Contrast. Following preprocessing, the functional time series for each run was high-pass filtered (65 s), intensity normalized to a whole brain mean of 10, 000 and spatially normalized by a 12-parameter affine transformation to Montreal Neurological Institute-152 atlas space.[43] We fit a general linear model (GLM) to the MR signal of each subject's preprocessed functional time series for each SIRP run to estimate the BOLD response associated with each memory set size for encode and probe periods within a run. The indicator coding of memory set conditions was convolved with a single gamma density distribution (σ = 3 s, delay to peak = 6 s or, equivalently, shape = 5.83, scale = 1.24) to produce 6 explanatory variables, one for each of the 3 memory set sizes associated with either encode or probe block periods. Encode and probe periods were modeled to separate the BOLD response to encoding events from the BOLD response to probes, which were the focus of the current study. The GLM also included temporal derivatives of the main explanatory variables to account for specific temporal shifts of the BOLD response that might vary over load level, event type, and run. Both linear and quadratic terms were included in the GLM to account for baseline drift.

The GLM produced 3 BOLD regression weights per run for the encode period. Each regression weight corresponded to the BOLD response of a single memory set size for encode or probe periods and did not themselves represent the effect of memory set size on the BOLD signal. In order to estimate the impact of memory set size, we applied standard polynomial contrast coefficients to the regression weights associated with each memory set.[44] Linear and quadratic contrasts of (regression) parameter estimates (ie, COPES) were derived for each participant and exhaustively accounted for the memory set size effect. The linear contrast compared the BOLD response for the 5-item memory set against the 1-item memory set, whereas the quadratic contrast compared the BOLD response for the 3-item memory set against the BOLD response to the other 2 memory set sizes. For each subject, the magnitude of the linear or quadratic COPE and an estimate of its variability derived from BOLD model residuals were passed to a second-level

analysis to combine COPES from separate runs, yielding a crossrun COPE value for each trend contrast.[45] The crossrun COPE values for the linear and quadratic memory set size trends were formed by the weighted sum of COPES from individual runs with the weights inversely proportional to the run-specific variation of each run's COPE value.[45] These crossrun linear and quadratic trends were correlated with the cognitive model parameters to test for group differences in correlations between BOLD response to increasing memory load and cognitive model parameters. Because the cognitive model parameters, described below, combined data from positive and negative trials, we did not model the BOLD signal separately for positive and negative probes.

RT Models. We developed 4 probability models to measure memory scanning speed in our RT data. Because error rates were so low (see below), accuracy was not modeled. We could have fit lines separately to the RT data from positive and negative trials to obtain 2 slope and 2 intercept parameters. The slope parameters would have been related to the memory scanning construct we sought to measure. If, however, the 2 slope parameters were different, we would have had to separately correlate the positive and negative slopes with BOLD variables or justify a scheme to combine the two slopes into a composite value. We would have also lost an opportunity to learn about the strategies our participants used to perform the SIRP. The models described below make specific a priori predictions about how the slopes of positive and negative trials should relate and elucidate different strategies participants might use to perform the task. Each of the models considered involved only 3 parameters and is more parsimonious than the 4-parameter, 2-slope/2-intercept model. The 4 models described below variously incorporated the ideas of exhaustive or self-terminating search and serial or parallel processing described in the introduction. As a group, the models possessed a broad theoretical scope and could fit a wide range of RT slopes (see figure 2). Although the group of models considered represented a broad range of theoretical ideas, specific models made commitments to specific constructs. By selecting the model with the best fit to our RT data, we were able to identify strategies participants used to perform the SIRP. The models are described next and in figure 3. Specific equations fit to the RT data can be obtained from the authors.

Serial Models: Exhaustive or Self-Terminating. Let υ_1 be the fraction of a memory set item successfully scanned per millisecond of processing when processing capacity is applied only to one item at a time and $\frac{1}{\upsilon_1}$ be the scan time for one item. If all the processing capacity is applied to one item until its scanning is completed before reallocating the capacity to the next item, the scanning process is serial.[8,9] When serial memory scanning exhaustively compares the target against all *k* items in a memory set before a response is made, the expected total RT, E(*T*), would be *k* times the scan time for one item plus an intercept. The intercept accounts for time taken to perform nonscanning processes, such as stimulus encoding, decision making, and response execution. This model is represented by model A in figure 3. The figure shows the assumed processing of a 3-parameter memory set {8 5 2} for a positive trial where the probe is 5. The first column in the figure shows a step where memory scanning of one of the digits in the memory set is completed. Column 2 shows which digits were scanned at a particular step, and column 4 indicates when the memory scanning process is terminated. The third column represents the presumed serial processing where the light gray triangle shows which digit is being scanned during each step. The main features of this model are the serial nature of the scanning and the completion of the scanning for all items in the memory set even when the target probe has already been scanned (see the second step). The exhaustive serial model includes one scanning capacity parameter, υ_1, and 2 intercept parameters—one for positive trials and one for negative trials.

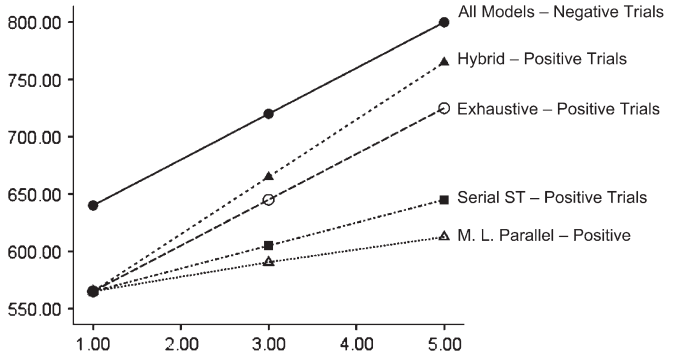

Fig. 2. Predicted Response Times by Memory Set Size for Each of 4 Retrieval Models (Hybrid, Serial Exhaustive, Serial Self-terminating, and a Moderately Limited Capacity [M.L.] Parallel Model). All models predict the same exhaustive search times for negative trials. Models predicted different slopes on positive trials. The positive intercept for the hybrid model has been set to equal the other models.

Plausibly, individuals might stop memory scanning on positive trials when they find a memory set item that matches the target.[9] If the position of targets in the memory set were to be randomly assigned, the self-termination of serial memory scanning on positive trials would be expected to occur on average after half of the items in the memory set were scanned.[9] On negative trials, individuals would always scan all items. Consequently, the ratio of negative to positive RT slopes would be 2:1. The self-terminating serial model is shown in figure 3B, where search is terminated after successfully scanning probe item 5 on the second step.

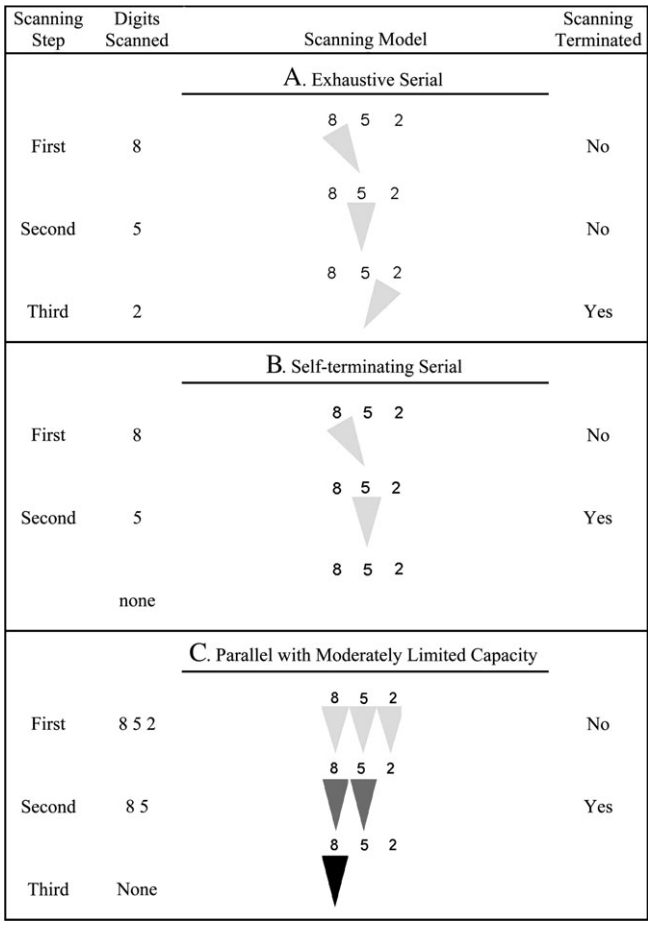

Fig. 3. Pictorial Representation of Memory Scanning During a Positive Trial as Postulated by Exhaustive Serial and Self-terminating Serial Models and by the Parallel Model With Moderately Limited Capacity and Stochastic Independence. A 3-item memory set {8 5 2} is assumed to be tested with the probe digit 5. The triangles in the figure show the direction of the memory scanning window, with darker trials representing greater memory scanning capacity and, hence, faster scanning speed. The digits scanned by a model at each completed scanning step is shown to the left of a scanning model. The right most column indicates when scanning is terminated. This figure represents only one of the possible paths, which depend on the order in which the probe is presented in the exhaustive and self-terminating models and on the momentary fluctuations in scanning efficiency in the parallel model with moderately limited capacity.

Like the exhaustive model, the self-terminating model involves one scanning capacity parameter and 2 intercepts.

Parallel Model With Moderately Limited Capacity and Stochastic Independence. The third model assumes at least as many processing channels as items in the memory set with each item processed by one channel. On the first processing step, let processing capacity be assigned equally to each channel, which operates in parallel and independently of the remaining channels. If the processing capacity is equal in each channel and unrelated to the number of channels, total processing capacity is unlimited because capacity can be increased by adding channels. If processing capacity in each channel is diminished as load increases, the system has moderately limited capacity.[8] By implication, the processing capacity for remaining items increases as the scan of an item is completed. These assumptions are represented in figure 3C where 3 channels process the 3 items in the memory set on the first step. In the figure, increased scanning capacity is represented by the increasingly darker triangles after successful scanning of a particular memory set item. This model predicts more rapid scanning slopes on positive trials than the serial models discussed above because processing capacity is augmented for subsequent items once processing of an item is complete. On the average, the ratio of negative to positive slopes predicted by this model is about 3:1.[8] As with the serial models, the model involves 1 scanning capacity parameter and 2 intercepts.

Two-Process Hybrid Model. The long 38-second probe period spanning 14 probes might have caused the mental representation of items included in the memory set to become corrupted. The hybrid model assumes that once memory scanning is complete for a particular probe, participants use the probe as a cue to retrieve the memory set from episodic memory. The search continues until the memory set retrieved matches the memory set scanned or until total search effort is exceeded. The search is assumed to be serial and self-terminating, implying that larger memory sets would take longer to retrieve. Computationally, the hybrid model subsumes the serial exhaustive model of memory scanning of figure 3A and a serial self-terminating model of memory search like figure 3B. Because the memory sets studied were small, search would generally be successful and terminated before the search effort was exceeded. Thus, the serial, self-terminating search process would add a second positive slope term to the slope term associated with memory scanning. For negative trials, the search process would generally proceed until it was exhausted. The effects of memory search, therefore, would be seen as a constant offset in the intercept on negative trials, with the slope on negative trials determined by the memory scanning rate and uninfluenced by the search rate. Because the effects of memory search on positive trials would be seen in the slope—determined by both the scanning capacity parameter υ_1 and the search capacity parameter υ_2—whereas the slope of the negative trials would be determined only by the scanning rate υ_1, the slopes of positive and negative trials would tend to converge. The intercept of the negative trials is assumed to be the positive trial intercept plus the time taken to exhaust memory search for the 5-item memory set. Thus, the hybrid model has 3 parameters: the scanning rate υ_1, the search rate υ_2, and the positive intercept.

Model Comparisons. All the models described above make the same prediction for the slope of negative trials; all models also have 3 parameters. As seen in figure 2 and discussed above, the models differ considerably when predicting the slopes of positive trials. Among the models considered, the hybrid model uniquely predicts a smaller slope on negative than positive trials because the positive slope is assumed to be determined by both υ_1 and υ_2 whereas the negative slope is determined only by υ_1. Moreover, the hybrid model predicts larger intercepts for negative trials rather than fitting separate positive and negative intercepts to RTs.

Statistical Analysis

Behavioral Data. Subjects were defined as being on task if they responded on at least 80% of the trials and responded correctly beyond chance levels on each run. The 80% cutoff was determined by plotting the number of trials completed in the group of healthy participants and using Tukey fencing rule to identify outliers.[46] Ten schizophrenia patients and 3 healthy comparison subjects were excluded from the study for not being on task. Most datasets dropped represented a failure to understand directions, such as responding only to positive targets, or reflected random responding. Individuals who were on task responded at high levels of accuracy when accuracy was measured as a percentage of trials where a response was recorded: healthy volunteers mean = 97.68 ± 2.74%, schizophrenia patients (SZ) = 95.42 ± 4.82%. An additional 3 patients and 7 healthy comparison subjects had behavioral data but no imaging data. These subjects were also omitted from the analysis.

We performed a fixed-effects analysis of variance to test for effects of group, memory set size, trial type, site, run, and their interactions on RTs. When violations of the sphericity assumption for repeated measures were detected, Huynh-Feldt fractional adjustments to degrees of freedom were made.[47]

Parameters Estimation and Model Selection. We used the simplex search method of Nelder and Mead to estimate parameters for each model.[48] Once parameters were estimated, a model generated predicted RTs for each memory set size, separately for positive and negative trials. These predicted values were compared with mean RTs for memory set size per trial type combination of each subject. We calculated the residual sums of squares and the Bayesian Information Criterion to assess the fit of a model's predicted RTs to observed mean RTs.[49] The Bayesian Information Criterion adds to a measure of the error in a model's fit a penalty term that increases as the number of parameters in the model increases.[49]

Correlating Model Parameters With Imaging Data. We used AFNI's 3dRegAna program to correlate model parameters voxel-wise with COPE maps within group and to test for group differences in the correlation of model parameters with COPE values for the linear and quadratic trends.[50] Because RTs have been found so consistently to be a linear function of increasing memory set size, we began with the assumption that scanning and search parameters would be linearly related to the brain's response to memory load. We investigated possible nonlinear relationships in exploratory analyses and in plots of residuals for selected brain regions, especially when correlating model parameters with the quadratic trend. Group differences in the correlation of a particular model parameter with BOLD response to memory load were tested using a regression model. Tests of the regression weight associated with an interaction term formed by the product of a dummy coding for group with a model parameter indicated whether the correlation of a model parameter with the BOLD value was significantly different between groups.[44] The model also included a dummy coding of magnet sites to control for mean site variation.[44] The importance of nuisance variables in moderating the relationship between a model parameter and BOLD response to memory load were also studied by including three way products involving group, the model parameter, and the nuisance variable. Three nuisance variables were studied: site, age, and predicted IQ. The importance of the nuisance variable was investigated by testing the change in R^2 associated with adding the nuisance variable.[44]

We used AFNI's AlphaSim simulation routine to identify a volume threshold to protect against detecting a large number of false positives during the voxel-wise analysis.[51] The cluster of correlations was considered to be significantly different from zero if the correlation in each voxel of the cluster was significantly different from zero at $P < .01$ and if adjacent significant voxels together formed a significance volume of at least 1893 mm^3. When calculating the significance volume, we assumed a smoothness of 8 mm, a connectivity radius requiring that the faces or edges of voxels touch to be considered adjacent, and a voxel-wise $P = .01$. Simulations indicated that under the null hypothesis of zero correlation within each brain voxel less than 5% of brains studied would show at least one false positive cluster that exceeded the significance volume threshold.[51]

Results

Subject Characteristics

Although healthy comparison subjects were significantly better educated than schizophrenia patients and had significantly greater projected IQs, the 2 groups did not differ on age, gender, handedness, or paternal education (see table 1). Patients displayed mild levels of negative symptoms of schizophrenia on the SANS with greater factor scores on apathy (2.25 ± 1.32) and anhedonia

Table 1. Demographic and Symptoms Findings: Mean (SD)

Variable	Schizophrenia Patients	Healthy Comparison
Subject's education (y)[a]	13.5 (2.00)	16.11 (2.15)
Paternal education (y)	14.09 (3.18)	15.00 (3.51)
Age (y)	37.95 (11.32)	35.99 (11.99)
NAART (estimated FIQ)[b]	105.64 (9.68)	112.64 (8.41)
Gender (% male)	67%	62%
Handedness (% right handed)	90%	89%

Note: NAART, North American Adult Reading Test.
[a]$P < .01$.
[b]$P < .001$.

(2.55 ± 1.42) than affective flattening (1.67 ± 1.54), inattention (1.30 ± 1.29), and alogia (1.10 ± 1.24).

Response Times

When averaged across load, stimulus type, run, and site, the RTs of schizophrenia patients were significantly slower than those of healthy controls (controls: 702 ± 129.53 ms, patients: 784 ± 125.82 ms, $F_{1,168} = 18.927$, $P < .001$, $\eta^2 = 0.11$). As seen in figure 4, schizophrenia patients had significantly larger slopes than healthy controls, indicating slower scanning times, $F_{1.8,295} = 8.182$, $P = .001$, $\eta^2 = 0.05$. The group difference in slope did not significantly interact with site, target type, or run (all $\eta^2 < 0.03$). Participants in both groups responded more slowly on negative than positive trials $F_{1,168} = 228.43$, $P < .001$, $\eta^2 = 0.58$. This disparity was significantly greater for schizophrenia patients compared with healthy participants $F_{1,168} = 10.87$, $P = .001$, $\eta^2 = 0.06$. The greater disparity between negative and positive RTs found among schizophrenia patients tended to normalize by the third run $F_{2,336} = 4.19$, $P = .016$, $\eta^2 = 0.024$. No other effects involving group were significant. Site, in particular, did not interact with group ($P = .865$, $\eta^2 = 0.019$).

Model Parameters

As seen in figure 4, the slopes of the positive and negative load curves were not parallel but rather tended to converge $F_{2,336} = 17.34$, $P < .001$, $\eta^2 = 0.09$. The finding of nonparallel slopes did not depend on group ($P = .667$, $\eta^2 = 0.004$). Only the hybrid model correctly predicts the observed converging pattern. Mean residual sums of squares and mean Bayesian Information Criterion values averaged over individuals within group confirm that the hybrid model fit RTs of both groups better than did the other 3 models (see table 2). We therefore report findings involving the hybrid model's memory scanning and memory search parameters. Schizophrenia patients experienced significantly slower memory scanning and memory search speeds (scan speed: $t_{181} = 2.91$, $P = .004$, 2-tailed, means ± SD: patients = 49.45 ± 21.25 ms; comparison subjects = 40.82 ± 18.75 ms; search speed: $t_{181} = 3.70$, $P < .001$, 2-tailed, means: patients = 23.59 ± 16.01 ms, comparison subjects = 15.88 ± 12.06 ms).

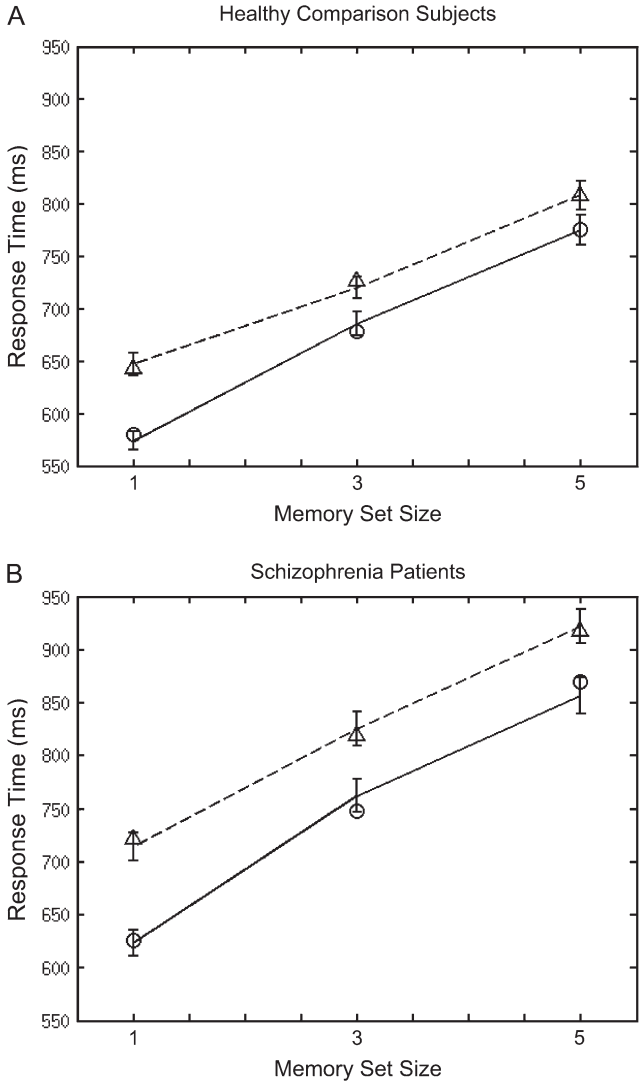

Fig. 4. Mean response times in milliseconds by memory set size for healthy comparison subjects and schizophrenia patients. Positive trials are displayed with a solid line and negative trials with a dotted line. Fitted Hybrid model values are represented by open circles for positive trials and open triangles for negative trials.

Correlation of Parameters With Activation Maps

The variance of memory scanning parameter values was significantly greater among schizophrenia patients than among healthy controls, $F_{1,181} = 3.93$, $P = .049$. Because the regression weights that we compared below would vary if the groups compared differed in their variances, even though the correlation coefficients were the same, we standardized parameter values to the same scale before proceeding with further analysis. The standardization was accomplished by performing a within group,

Table 2. Model Fits

Model	Mean Residual Sums of Squares		Mean Bayesian Information Criterion	
	Healthy Participants	Schizophrenia Patients	Healthy Participants	Schizophrenia Patients
Exhaustive serial	380.92	522.03	30.28	32.17
Self-terminating Serial	5724.23	6998.42	46.54	47.75
Parallel MoLCSI	10 653.69	13 703.51	50.27	51.78
Hybrid	13.82	502.64	10.38	31.94

Note: Parallel MoLCSI is parallel moderately limited capacity with stochastic independence.

normalizing, rank to *z* transformation of the memory scanning and memory search speeds.[44,52]

Within each group, the hybrid model's memory scanning and search parameters were separately correlated with the linear and quadratic trends that represented the BOLD response to increasing memory load for probe events. Group differences in the correlation of the scan parameter with the linear memory load were observed in multiple cortical and subcortical sites (table 3). Areas of group differences in correlation were observed in the (1) right precuneus extending subcortically to the tail of the right caudate nucleus, (2) left middle frontal gyrus extending toward the head of the caudate nucleus, (3) left inferior frontal gyrus extending to the head of the caudate, (4) bilateral caudate, and (5) the right frontopolar gyrus. Group differences in the correlation of the scan parameter with the quadratic memory load trend were observed in an area encompassing the left entorhinal and perirhinal cortex and the anterior parahippocampal gyrus and in the right postcentral and precentral gyri (table 3 and figure 5). Generally, the 3-way interaction of group, scan parameter value, and site was not significant in any of the areas listed in table 3, indicating that site differences did not significantly mediate the group differences in correlations we observed. Two exceptions were the finding of a 3-way interaction in the tail of the right caudate for the linear memory load trend and a 3-way interaction in the right postcentral gyrus for the quadratic memory load trend.

There was no brain area where a group difference in correlation of the search parameter with the linear trend was significant at the cluster volume threshold that we set. Two regions in the right middle frontal cortex did show group differences in the pattern of correlation of speed of memory search with the quadratic BOLD response to increasing memory load (table 4).

In all the areas where group differences in correlations were found, the correlations of healthy volunteers were positive and larger than among patients with schizophrenia. The pattern of memory scanning correlation in the left inferior frontal gyrus for the linear trend and in the left entorhinal/perirhinal cortex for the quadratic trend are plotted in figure 6. The plot in figure 6A suggests that healthy participants who scanned the memory set more slowly experienced their largest BOLD response to the highest memory load compared with

Table 3. Cortical Regions With Differential Correlations of the Memory Scanning Parameter With Brain Response to Increasing Working Memory Load

BOLD Response to Memory Load	Anatomical Location	Talairach Coordinates	Pattern of Correlation Difference
Linear	L middle frontal gyrus extending toward the head of the caudate and to the left insula	34L, 26A, 26S	HV > Sz
Linear	L inferior frontal gyrus extending to the head of the caudate	34L, 26A, 8I	HV > Sz
Linear	R precuneus extending to the tail of the R caudate	24R, 66P, 34S	HV > Sz
Linear	Bilateral caudate	14R, 2P, 16S; 12L, 20A, 2S	HV > Sz
Linear	Bilateral, primarily R frontopolar gyrus	6R, 54A, 16S	HV > Sz
Quadratic	L entorhinal cortex including perirhinal and anterior parahippocampal gyrus	20L, 10P, 26I	HV > Sz
Quadratic	R postcentral gyrus extending to R precentral gyrus and to R superior parietal lobe	68R, 16P, 22S	HV > Sz

Note: L = left, A = anterior, S = superior, HV = healthy volunteers, Sz = schizophrenia patients, I = inferior, R = right, P = posterior.

Table 4. Cortical Regions With Differential Correlations of the Memory Search Parameter With Brain Response to Increasing Memory Load

BOLD Response to Memory Load	Anatomical Location	Talairach Coordinates	Pattern of Correlation Difference
Quadratic	R middle frontal gyrus extending into the R inferior frontal gyrus	40R, 12A, 26S	HV > Sz
Quadratic	R middle frontal gyrus separate from and anterior to the cluster above	30R, 34A, 26S	HV > Sz

Note: BOLD, blood oxygen level–dependent, R = right, A = anterior, S = superior, HV = healthy volunteers, Sz = schizophrenia.

healthy participants who scanned more quickly (see red line). This relationship appears attenuated among schizophrenia patients (see blue line). Regression analyses supported this impression with the relationship between scanning speed and the linear BOLD response in the left inferior frontal gyrus significant only among healthy participants, $F_{1,92} = 13.273$, $P < .001$, $r = 0.36$. This pattern of significant, positive correlations between scanning speed and linear BOLD response among healthy volunteers coupled with nonsignificant correlations among schizophrenia patients was also observed in the left middle frontal gyrus, bilateral caudate, right precuneus, and frontopolar cortex.

Interpreting the relationship between scanning speed and the quadratic response to increasing memory load in the entorhinal/perirhinal cortex was more complex. Healthy volunteers who scanned the memory set fastest tended to show a smaller quadratic BOLD response to memory load, whereas healthy controls who scanned more slowly displayed a larger quadratic response; patients displayed the opposite pattern figure 6B. Regression analyses confirmed this cross-over pattern: healthy controls, $F_{1,92} = 4.74$, $P = .032$, $r = 0.22$; schizophrenia patients, $F_{1,80} = 31.13$, $P < .001$, $r = -0.53$. Inspection of mean BOLD response to each memory set size in the perirhinal and entorhinal cortex cluster revealed negative BOLD responses to probes for all memory set sizes. The pattern for fast healthy controls revealed near zero BOLD response to memory sets with one digit and larger degrees of inhibition for the memory sets with 3 or 5 digits. Slow scanning healthy controls showed a large degree of inhibition only for the largest set size. Fast responding patients with schizophrenia showed the same pattern as slow responding controls, whereas the slow scanning schizophrenia patients showed greater overall inhibition with the largest negative BOLD response appearing during probes at the intermediate memory load.

We investigated whether age or projected IQ mediated the group difference in correlation pattern between scanning speed and BOLD response to memory load in the frontal areas central to our hypothesis and in the left perirhinal/entorhinal cluster. Neither age nor estimated IQ had a mediational effect in theses areas. We also tested the assumption that the relationship between scanning speed and BOLD response to memory load was linear by adding a quadratic memory scanning predictor to the analysis model. Adding a quadratic memory scanning term did not improve the analysis model's fit to the BOLD memory load response in inferior frontal, middle frontal, or perirhinal/entorhinal clusters.

Discussion

Performance on the serial item recognition test was best accounted for by a probability model that included both memory scanning and memory search parameters. Of the models explored, only the hybrid retrieval model correctly predicted the convergence of RT slopes for negative and positive trials across increasing memory set sizes. The model also correctly predicted the larger intercepts observed in the negative trials. The converging slope is not typically reported in memory scanning studies of patients with schizophrenia.[25–27] Its occurrence in this study might have been related to the relatively lengthy probe period employed, adding a memory search term as described by the hybrid model. Additionally, earlier studies involved considerably smaller sample sizes lessening the statistical power to detect subtle slope differences.

Group differences were found in the correlation of memory scanning speed with linear increases in BOLD response to increasing memory load during the probe period. These differential patterns of correlation were found in left dorsal and ventral PFC, confirming the study's main hypothesis, and included the caudate nucleus. The results are compatible with the finding of abnormal brain response in the PFC and basal ganglia among patients with schizophrenia performing the SIRP.[20] The present results extend the previous group analysis by showing that abnormal patterns of correlation between scanning speed and BOLD response to memory load occur in PFC and caudate of patients with schizophrenia. Studies of the frontocaudate network in working memory have implicated the PFC, especially the ventral PFC, in the maintenance of information with the caudate involved in executive aspects of WM.[54,55] Given the hypothesized contribution of the caudate to executive aspects of WM, caudate activity might contribute to the interface between the scanning and decision-making processes involved in the SIRP. We also observed a differential pattern of correlation between memory

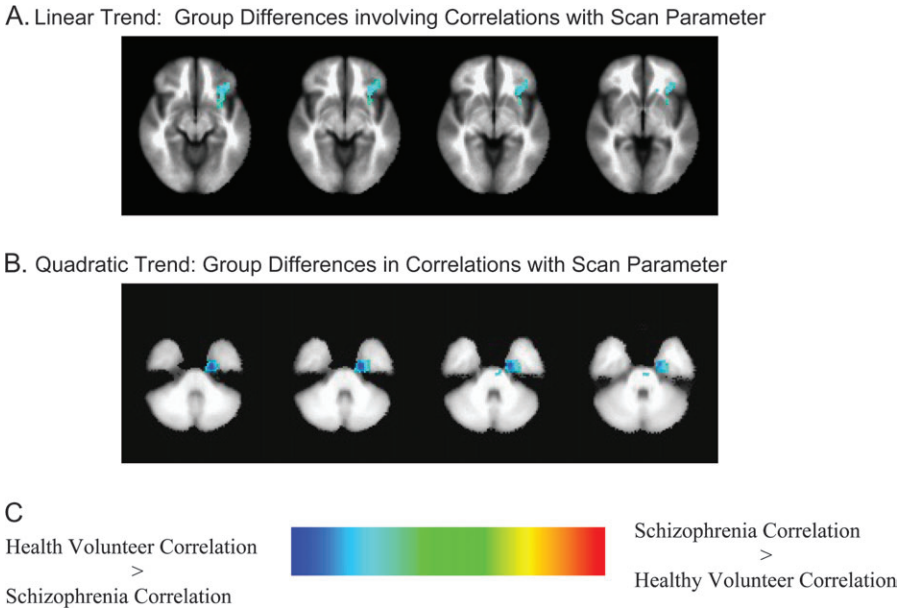

Fig. 5. (A) Group differences in correlations between the linear BOLD response to increasing memory load for probe events and the Hybrid model memory scanning. (B) Group differences in correlations between the quadratic BOLD response and memory scanning in the left perirhinal/entorhinal cortex. (C) Group differences in the correlations between the quadratic BOLD response and the hybrid model search parameter in the right postcentral gyrus. Values are regression weights for the interaction of group with the memory scanning or search parameter. Cool colors indicate that the correlation associated with healthy volunteers is greater than the correlation associated with patients. Hot colors indicate the opposite pattern.

scanning speed and the linear BOLD response to memory load in the right precuneus. This region participates in the allocation of spatial attention to the perception of numbers and their relative locations[56] and, in our data, appears to be involved in accounting for individual differences in scanning speed among healthy volunteers.

Given inconsistencies in prior studies regarding lateralized PFC activation during SIRP performance and its differences between groups,[2,20] we did not have clear a priori hypotheses regarding laterality. In the present study, group differences in correlation of memory scanning with brain activity showed significant effects only in the left PFC. A possible interpretation of this finding is that one strategy by which digits are actively maintained in WM is covert verbal rehearsal as was suggested by Sternberg in his original work.[63] Rehearsal might have engaged left PFC more strongly and been more critical at higher loads, accounting for the association of slower scanning speed with greater activation at higher loads we observed among healthy participants. It should be noted that the literature concerning PFC specialization by material type is controversial (for review, see D'Esposito et al, 1998),[64] and other aspects of performance may have accounted for hemispheric differences.

In areas where group differences in the correlation between the scanning parameter and the linear BOLD response to memory load were found, healthy volunteers with faster scanning speeds also showed less activation of BOLD response as the memory set size increased. Together, the behavioral and brain data imply that fast scanning healthy volunteers require little additional neurocognitive capacity to scan working memory when scanning load is increased. Slower scanning, healthy participants showed linear increases in BOLD response to increasing scanning load. Unlike healthy participants, patients with schizophrenia showed an uncoupling of performance to brain response in the PFC and caudate as memory load increased.

Interpreting correlations involving the quadratic BOLD response to increasing memory load was more complex. A detailed analysis of the differential group patterns of scanning speed with the quadratic BOLD trend revealed a cross-over pattern of correlation. Examination of the BOLD response during the probe period to each memory load revealed a consistent pattern of negative BOLD values for all conditions in both groups. The BOLD response to a probe of a memory set of a particular size compared brain activity during the presentation of an item probe with the BOLD responce to a fixation cross. It is reasonable, therefore, to hypothesize that the negative BOLD response was due to neural inhibition rather than to the activating potency of the fixation stimulus. Interestingly, there is considerable animal and human evidence to support the hypothesis that neural function in the perirhinal cortex is inhibited during recognition memory probes.[57,58] In some theories, the inhibition can have a cascading effect, reducing neural activity in nearby entorhinal and anterior parahippocampal cortex.[57] Assuming that the negative BOLD response was due to inhibition during the memory probe period rather than to

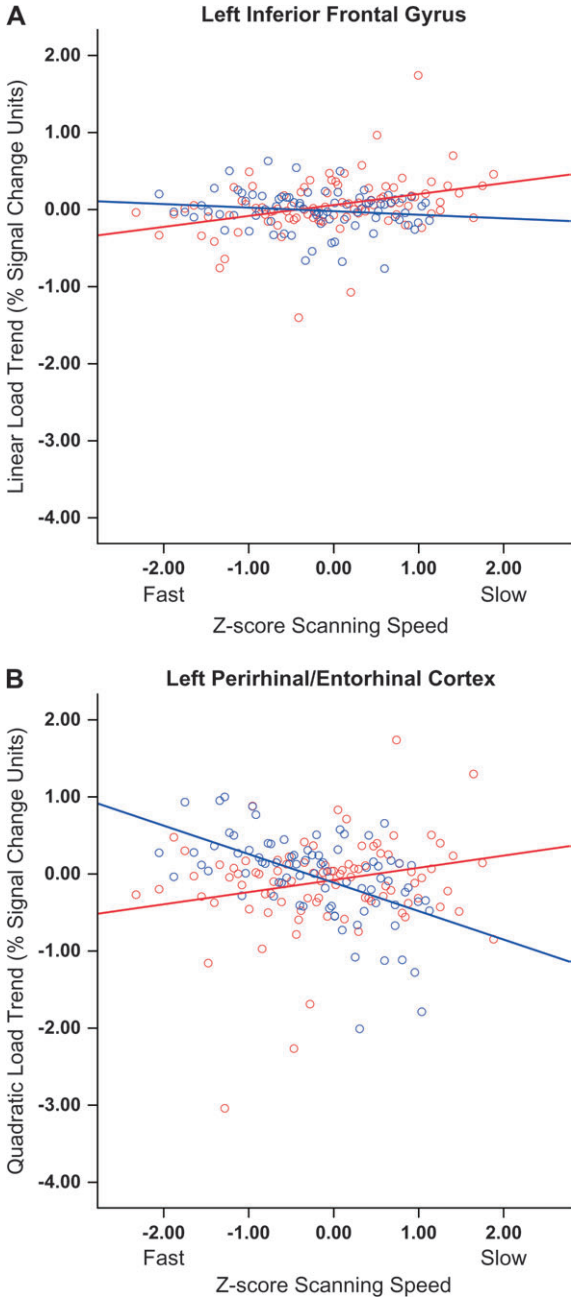

Fig. 6. (A) Correlation of the *Z*-score transform of the memory scanning parameter with the linear BOLD response to increasing memory load (percent signal change units) in the left inferior frontal cortex. (B) Correlation of the Z-score transform of the memory scanning parameter with the quadratic BOLD response to increasing memory load (percent signal change units) in the left perirhinal/entorhinal cortex. Negative Z-scores indicate faster scanning speeds. Red line: Healthy volunteers; Blue line: Schizophrenia patients.

activation during the fixation condition, an interesting pattern of inhibition appeared in the results. Fast scanning healthy controls showed an augmented inhibitory response to memory sets containing 3 or 5 digits. Slow scanning healthy controls showed an augmented inhibitory response that appeared only when 5-item memory sets were probed. Fast responding patients with schizophrenia showed a pattern of inhibitory augmentation very similar to slower scanning healthy participants. Slow scanning patients showed a disordered pattern of inhibition that was present even during probes of the smallest memory set, crested when 3 digits were probed, and declined during the 5 probe set.

The study findings depend in part on which model best fit the data. The extent to which the pattern of correlations would differ if models other than the hybrid model were selected could only be determined by correlating parameters from each of the proposed models with brain activity. Given that the core study findings involved a memory scanning parameter, derived from the exhaustive search component of the hybrid model, it is possible that similar findings would have been obtained had the scanning parameter of the exhaustive serial model been correlated with BOLD response (figure 3A). Yet, the evidence for the hybrid model was reasonably strong. It not only fit the RTs of both groups better than the other models, it also was the only model that predicted converging slopes for positive and negative trials, a finding that appeared in both groups. Moreover, the mean scanning time estimated for healthy participants, 40.82 milliseconds, was similar to what has been reported among healthy individuals,[9] while the mean search time, 15.88 milliseconds, was similar to times from recognition memory studies.[59,60] We did not directly test the hypothesis that the memory search process served to recheck the veridicality of the scan decision before it was emitted. Rather, the notion of rechecking was taken from the theories of lexical activation, another high-speed cognitive process. Studies directly comparing mechanisms underlying recognition memory and lexical activation support the plausibility of theories that postulate common cognitive mechanisms.[61,62] Although our application of rechecking to memory scanning is plausible, it requires further verification.

As with many voxel-wise brain-imaging analyses, the analysis in this article was exploratory. The results from this study need to be replicated before definite conclusions can be reached. This is particularly important given that the observed correlations generally varied in the +0.45 to –0.45 range. Whether different probability models fit different subgroups of schizophrenia patients needs to be explored in more detail. Exploratory analyses aimed at identifying subgroups of schizophrenia patients might be initially pursued in a cluster analysis that included scanning model parameters, functional brain images, and clinical data. The findings from our study might be limited by the specific SIRP task used. Our version included a long probe period that was efficient in obtaining brain activity data during the probe period, yet might have introduced cognitive processes not usually associated with memory scanning into the task. Finally, our study only examined WM processes involved in accessing information maintained over short periods in the face of distraction. It

adds little new information about how schizophrenia might influence other WM processes, such as strategic shifts of attention, information manipulation, episodic memory encoding, and maintenance of WM span. Study results are specific to the scanning of simple verbal stimuli and to patients with chronic schizophrenia.

Our data indicate that among individuals with schizophrenia, memory scanning speed is uncoupled from the brain's response to increasing WM load in the PFC and caudate nuclei. Moreover, schizophrenia patients show either an inefficient or disordered pattern of inhibition as WM load increases in the left perirhinal/entorhinal cortex. These results are compatible with neither a simple inefficiency model nor a simple deficit model. They do show that variations in the severity of cognitive function among individuals with schizophrenia appear to involve a disordered pattern of activation and inhibition among several brain regions, even when performing a task as simple as memory scanning.

Funding

National Center for Research Resources to the Function Biomedical Informatics Research Network (National Institutes of Health grant 1 U24 RR021992); Department of Veterans Affairs Mental Illness Research Education and Clinical Center grant to the Desert Pacific Healthcare System.

References

1. Egan MF, Weinberger DR. Neurobiology of schizophrenia. *Curr Opin Neruobiol*. 1997;7:701–707.
2. Manoach DS, Press DZ, Thangaraj V, et al. Schizophrenic subjects activate dorsolateral prefrontal cortex during a working memory task, as measured by fMRI. *Biol Psychiatry*. 1999;45:1128–1137.
3. Zorrilla LT, Jeste DV, Brown GG. Functional MRI and novel picture-learning among older patients with chronic schizophrenia: abnormal correlations between recognition memory and medial temporal brain response. *Am J Geriatr Psychiatry*. 2002;10:52–61.
4. Zarahn E, Aguirre G, D'Esposito M. A trial-based experimental design for fMRI. *Neuroimage*. 1997;6:122–136.
5. Friston KJ, Fletcher P, Josephs O, Holmes A, Rugg MD, Turner R. Event-related fMRI: Characterizing differential responses. *Neuroimage*. 1998;7:30–40.
6. McKeown MJ, Makeig S, Brown GG, et al. Analysis of fMRI data by blind separation into independent spatial components. *Hum Brain Mapp*. 1998;6:160–188.
7. Calhoun VD, Kiehl KA, Pearlson GD. Modulation of temporally coherent brain networks estimated using ICA at rest and during cognitive tasks. *Hum Brain Mapp*. 2008;29:828–838.
8. Townsend JT, Ashby FG. *Stochastic Modeling of Elementary Psychological Processes.* New York, NY: Cambridge University Press; 1983.
9. Sternberg S. Memory scanning: new findings and current controversies. In: Deutsch D, Deutsch JA, eds. *Short-term Memory.* New York, NY: Academic Press; 1975:195–231.
10. Goldman-Rakic PS. Prefrontal cortical dysfunction in schizophrenia: the relevance of working memory. In: Carroll BJ, Barrett JE, eds. *Psychopathology and the Brain.* New York, NY: Raven Press; 1991:1–23.
11. Cohen JD, Braver TS, O'Reilly RC. A computational approach to prefrontal cortex, cognitive control and schizophrenia: recent developments and current challenges. *Philos Trans R Soc Lond B Biol Sci*. 1996;351:1515–1527.
12. Keefe RS. Working memory dysfunction and its relevance to schizophrenia. In: Sharma T, Harvey PD, eds. *Cognition in Schizophrenia: Impairments, Importance, and Treatment Strategies.* New York, NY: Oxford University Press; 2000:16–50.
13. Barch DM, Carter CS, Braver TS, et al. Selective deficits in prefrontal cortex function in medication-naive patients with schizophrenia. *Arch Gen Psychiatry*. 2001;58:280–288.
14. Green MF. What are the functional consequences of neurocognitive deficits in schizophrenia? *Am J Psychiatry*. 1996;153:321–330.
15. Liddle PF. Cognitive impairment in schizophrenia: its impact on social functioning. *Acta Psychiatr Scand*. 2000;101:11–16.
16. Cannon TD, Huttunen MO, Lonnqvist J, et al. The inheritance of neuropsychological dysfunction in twins discordant for schizophrenia. *Am J Hum Genet*. 2000;67:369–382.
17. Conklin HM, Curtis CE, Katsanis J, Iacono WG. Verbal working memory impairment in schizophrenia patients and their first-degree relatives: evidence from the digit span task. *Am J Psychiatry*. 2000;157:275–277.
18. Park S, Holzman PS, Goldman-Rakic PS. Spatial working memory deficits in the relatives of schizophrenic patients. *Arch Gen Psychiatry*. 1995;52:821–828.
19. Manoach DS. Prefrontal cortex dysfunction during working memory performance in schizophrenia: reconciling discrepant findings. *Schizophr Res*. 2003;60:285–298.
20. Manoach DS, Gollub RL, Benson ES, et al. Schizophrenic subjects show aberrant fMRI activation of dorsolateral prefrontal cortex and basal ganglia during working memory performance. *Biol Psychiatry*. 2000;48:99–109.
21. Atkinson RC, Juola JF. Search and decision processes in recognition memory. In: Krantz DH, Atkinson RC, Luce RD, Suppes P, eds. *Contemporary Developments in Mathematical Psychology, Vol. 1: Learning, Memory, and Thinking.* San Francisco, Calif: WH Freeman and Company; 1974:243–293.
22. Neely JH, Keefe DE, Ross KL. Semantic priming in the lexical decision task: roles of prospective prime-generated expectancies and retrospectic semantic matching. Journal of experimental psychology. *J Exp Psychol Learn Mem Cogn*. 1989;15:1003–1019.
23. Neufeld RWJ, Vollick D, Highgate S. Stochastic modeling of stimulus encoding and memory search in paranoid schizophrenia: clinical and theoretical implications. In: Cromwell RL, Snyder CR, eds. *Schizophrenia: Origins, Processes, Treatment, and Outcome.* New York, NY: Oxford University Press; 1993:176–196.
24. Korboot P, Yates AJ. Speed of perceptual functioning in chronic non-paranoid schizophrenics: partial replication and extension. *J Abnorm Psychol*. 1973;81:296.
25. Sternberg S. Memory scanning: New findings and current controversies. In: Deutsch D, Deutsch JA, eds. *Short-term Memory.* New York, NY: Academic Press; 1975:195–231.
26. Koh SD, Szoc R, Peterson RA. Short-term memory scanning in schizophrenic young adults. *J Abnorm Psychol*. 1977;86:451.

27. Wishner J, Stein MK, Penstral AL. Stages of information processing in schizophrenia: Sternberg's paradigm. In: Wynne LC, Cromwell RL, Matthysse S, eds. *The Nature of Schizophrenia: New Approaches to Research and Treatment.* John Wiley & Sons: New York, NY; 1978.
28. Marusarz TZ, Koh SD. Contextual effects on the short-term memory retrieval of schizophrenic young adults. *J Abnorm Psychol*. 1980;89:683.
29. Russell PN, Consedine CE, Knight RG. Visual and memory search by process schizophrenics. *J Abnorm Psychol*. 1980;89: 109–114.
30. American Psychiatric Association.*Diagnostic and Statistical Manual of Mental Disorders – Fourth Edition 2000;Arlington, VaAmerican Psychiatric Association.*
31. Blair JR, Spreen O. Predicting premorbid IQ: a revision of the National Adult Reading Test. *Clin Neuropsychol*. 1989;3: 129–136.
32. First MB, Spitzer RL, Williams JBW. *Structural Clinical Interview for DSV-IV-TR Axis I Disorders, Research version, Patient Edition With Psychotic Screen (SCID-I/P W/PSY SCREEN)*. New York: Biometrics Research, New York State Psychiatric Institute; 2002.
33. McFarland K, Anderson J. Factor stability of the Edinburgh Handedness Inventory as a function of test-retest performance, age and sex. *Br J Psychol*. 1980;71:135–142.
34. Hollingshead AB. *Four factor index of social status.* New Haven, Conn: Yale University; 1975. Unpublished manuscript.
35. Guy W. *ECDEU Assessment Manual for Psychopharmacology-Revised (DHEW Publ No ADM 76-338)*. Rockville, Md: U.S. Department of Health, Education, and Welfare, Public Health Service, Alcohol, Drug Abuse, and Mental Health Administration, NIMH Psychopharmacology Research Branch, Division of Extramural research Programs; 1976:534–537.
36. Andreasen NC, Arndt S, Miller D, Flaum M, Nopoulos P. Correlational studies of the Scale for the Assessment of Negative Symptoms and the Scale for the Assessment of Positive Symptoms: an overview and update. *Psychopathology*. 1995;28:7–17.
37. Reber PJ, Wong EC, Buxton RB, Frank LR. Correction of off resonance-related distortion in echo-planar imaging using EPI-based field maps. *Magn Reson Med*. 1998;39:328–30.
38. www.sdsc.edu/srb/index.php/Main_Page. Accessed October 29, 2008.
39. http://nifti.nimh.nih.gov. Accessed October 29, 2008.
40. www.fmrib.ox.ac.uk. Accessed October 29, 2008.
41. Friedman L, Glover GH, Krenz D, Magnotta V. The FIRST BIRN Reducing inter-scanner variability of activation in a multicenter fMRI study: role of smoothness equalization. *Neuroimage*. 2006;32:1656–1668.
42. http://surfer.nmr.mgh.harvard.edu. Accessed October 29, 2008.
43. Carmack PS, Spence J, Gunst RF, Schucany WR, Woodward WA, Haley RW. Improved agreement between Talairach and MNI coordinate spaces in deep brain regions. *Neuroimage*. 2004;22:367–371.
44. Cohen J, Cohen P, West SG, Aiken LS. *Applied Multiple Regression/Correlation Analysis for the Behavioral Sciences.* (3rd ed). Mahway, NJ: Lawrence Erlbaum Associates; 2003.
45. Beckmann FC, Jenkinson M, Smith SM. General multilevel linear modeling for group analysis in FMRI. *Neuroimage*. 2003;20:1052–1063.
46. Tukey JW. *Exploratory Data Analysis.* Reading, Mass: Addison-Wesley Pub. Co; 1977.
47. Winer BJ, Brown DR, Michels KM. *Statistical Principles in Experimental Design.* 3rd ed New York, NY: McGraw Hill; 1991.
48. Nelder JA, Mead R. A simplex method for function minimization. *Comput J*. 1965;7:308–313.
49. Schwartz G. Estimating the dimension of a model. *Ann Statistics*. 1978;6:461–464.
50. http://afni.nimh.nih.gov/pub/dist/doc/program_help/3dRegAna.html. Accessed October 29, 2008.
51. http://afni.nimh.nih.gov/pub/dist/doc/program_help/AlphaSim.html. Accessed October 29, 2008.
52. Kerlinger FN, Pedhauzur EJ. *Multiple Regression in Behavioral Research.* New York, NY: Holt, Rinehart and Winston, Inc; 1973.
53. Manoach DS, Greve DN, Lindgren KA, Dale AM. Identifying regional activity associated with temporally separated components of working memory using event-related functional MRI. *Neuroimage*. 2003;20:1670–1684.
54. Lewis SJ, Dove A, Robbins TW, Barker RA, Own AM. Striatal contributions to working memory: a functional magnetic resonance imaging study in humans. *Eur J Neurosci*. 2004; 19:755–760.
55. D'Esposito M. Functional neuroimaging of working memory. In: Cabeza R, Kingstone A, eds. *Handbook of Functional Neuroimaging of Cognition.* Cambridge, Mass: The MIT Press; 2001:293–327.
56. Zago L, Petit L, Turbelin MR, Andersson F, Vigneau M, Tzourio-Mazoyer N. How verbal and spatial manipulation networks contribute to calculation: an fMRI study. *Neuropsychologia*. 2008;46:2403–2414.
57. Diana RA, Yonelinas AP, Ranganath C. Imaging recollection and familiarity in the medial temporal lobe: a three-component model. *Trends Cogn Sci*. 2007;11:379–386.
58. de Curtis M, Paré D. The rhinal cortices: a wall of inhibition between the neocortex and the hippocampus. *Prog Neurobiol.* 2004;74:101–110.
59. Flexner AJ. Long-term recognition latencies under rehearsal-controlled conditions: do list-length effects depend on active memory? *J Exp Psych: Hum Learn Mem*. 1978;4:47–54.
60. Burrows D, Okada R. Memory retrieval from long and short lists. *Science*. 1975;188:1031–1033.
61. Connor LT, Balota DA, Neely JH. On the relation between feeling of knowing and lexical decision: persistent subthreshold activation or topic familiarity? *J Exp Psychol Learn Mem Cogn*. 1992;18:544–554.
62. Yaniv I, Meyer DE. Activation and metacognition of inaccessible stored information: potential bases for incubation effects in problem solving. *J Exp Psychol: Learn Mem Cogn*. 1987; 13:187–205.
63. D'Esposito M, Aguirre GK, Zarahn E, Ballard D, Shin RK, Lease J. Functional MRI studies of spatial and nonspatial working memory. *Cogn Brain Res.* 1998;7:1–13.
64. Sternberg S. High-speed mental scanning in human memory. *Science*. 1966;153:652–654.
65. http://www.pstnet.com/products/SRBOX/default.htm.Accessed October 29, 2008.
66. Callicott JH, Mattay VS, Verchinski BA, Marenco S, Egan MF, Weinberger DR. Complexity of prefrontal cortical dysfunction in schizophrenia: more than up or down. *Am J Psychiatry*. 2003;160:2209–2215.
67. Simpson GM, Angus JW. A rating scale for extrapyramidal side effects. *Acta Psychiatr Scand Suppl*. 1970;212:11–19.
68. Barnes TR. A rating scale for drug-induced akathisia. *J Psychiatry*. 1989;154:672–676.